BULLETIN OF THE POLISH ACADEMY OF SCIENCES
TECHNICAL SCIENCES
Vol. 54, No. 1, 2006

# Moving from micro- to nanoworld in optical domain scanning probe microscopy

J. RADOJEWSKI*

Faculty of Microsystem Electronics and Photonics, Wrocław University of Technology, 11/17 Janiszewskiego St., 50-372 Wrocław, Poland

**Abstract.** In the article we described the evolution of optical technology from lens-type microscopes working in far-field to SNOM (Scanning Near-Field Optical Microscopy) constructions. We considered two systems elaborated in our laboratory, namely PSTM system (Photon Scanning Tunelling Microscope) and SNOM system. In both systems we obtained subwavelength resolution. Some details about optical point probe technology in both systems are given and experimental results presented.

**Key words:** optical Microscopy, PSTM, SNOM, tip technology, piezoresistive cantilever.

## 1. Introduction

The optical microscopy was invented some 350 years ago. It started from 30× magnification as it was stated by Robert Hooke [1] in early reports of microscope investigations. During the nineteenth century microscope constructors overcame the main problem at that time – lens aberrations and since then optical microscopy became an important scientific technique and was used in many applications in biology, material science and chemistry. In general, microscopes based on lenses, as mentioned above, are far-field optical instruments in which the imaging element – the lens – is placed many wavelengths away from the object under observation. In that case, when the system is aberrations free, the minimum size of focused optical beam i.e. lateral resolution is determined by diffraction from the limiting aperture of the optical system. This was stated first by Abbe in his famous work on diffraction and microscopic imaging [2]. He noticed that due to limited aperture of lenses, only limited part of angular spectra of propagating light could be collected. He came up with a so-called point-spread-function (PSF), which gives the intensity distribution in the image plane due to point source in the object plane. Rayleigh stated that objects could be resolved when maximum of the intensity distribution of one point source is in the same place then first minimum of the other point source (Fig. 1).

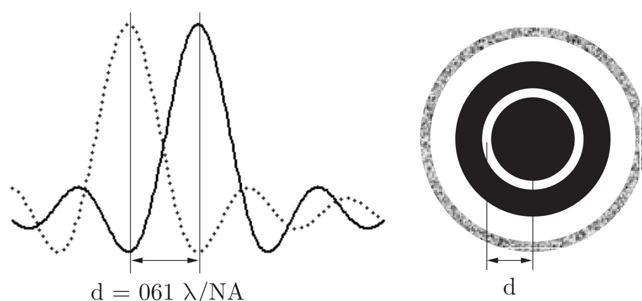


Fig. 1. Rayleigh difraction limit illustration

This is called Rayleigh diffraction limit [3]:

$$d = 0.61\lambda/NA$$

where: $d$ – is distance between distinguishable objects, $\lambda$ – is light wavelength, $NA$ – is numerical aperture.

The above formula is valid only for non-coherent point light emitters, observed by diffraction limited lens system. The easiest way to increase the resolving power is in this case increasing of $NA$ or decrease of light wavelength. In practice maximum $NA$ is about 0.4–0.5 (in air), and for optical microscope light wavelength should be within visible light spectrum. In practice the absolute resolution is equal to one half of the light wavelength and is roughly 250 nm. Of course there are a few methods used to obtain higher resolution images by utilization of shorter wavelength radiation (high energy electrons. X-rays ) but they are destructive, not so cheap, fast and easy to use as an optical methods. The way to increase resolution and contrast in optical domain was found by Minsky, who patented his invention in 1957. It is called scanning confocal microscopy. The image obtained in conventional optical microscopy suffers from the out-of-focus light reflected from features above and below the focal plane. In scanning confocal microscopy however by using pinhole screens – one near light source and second near detector, contribution of out-of-focus light is reduced $1/z^2$ times (z is the distance to the focal plane), so background and stray-light is almost absent in the image [4]. The 1.4 time improvement of the lateral resolution is also achieved because now the outcome PSF distribution in detector plane is the product of the illuminating beam and the pinhole PSF distribution [5]. Further resolution improvement in lens type microscopy is still being made by using special geometries of illumination and detection, and nonlinear effects such as two- or multiphoton excitation, but progress is very slow and no major steps forward are to be expected. Techniques which enable overcoming diffraction limit barriers in optical domain microscopy are presented below.

*e-mail: jacek@radojewski.net

## 2. Breaking diffraction limit – scanning near-field optical microscopy (SNOM)

The first concept of near-field optical microscopy (SNOM) was published by Synge [6] in 1928. The idea is conceptually very simple. Following this idea, it is enough to produce a light source with dimensions much smaller then light source wavelength and place it close to the sample surface in near-field region. Then the source should be raster scanned over the surface with simultaneously recorded transmitted or/and reflected optical signal. In 1984 Pohl at al. [7] and Lewis at al. [8] demonstrated this technology practically. Nowadays it offers different possibilities for topographic, optical and spectroscopic measurements. To name a few: fluorescence (specially in biological applications [9,10]), Raman and IR spectroscopy [11,12] and polarization contrast ( optical anisotropy, electron spin dynamics, magneto-optical phenomena [13,14]) There are a few common types of scanning near-field optical microscopy illustrated in Fig. 2. In our laboratories at Faculty of Microsystem Electronics and Photonics we developed two kinds of SNOM:

— PSTM type (based on construction from [15]) utilizing tapered monomode waveguides as a probe,
— SNOM in transmission mode with micromachined Si cantilevers of our construction with apertures fabricated on the very end of metal tip located at the end of silicon cantilever.

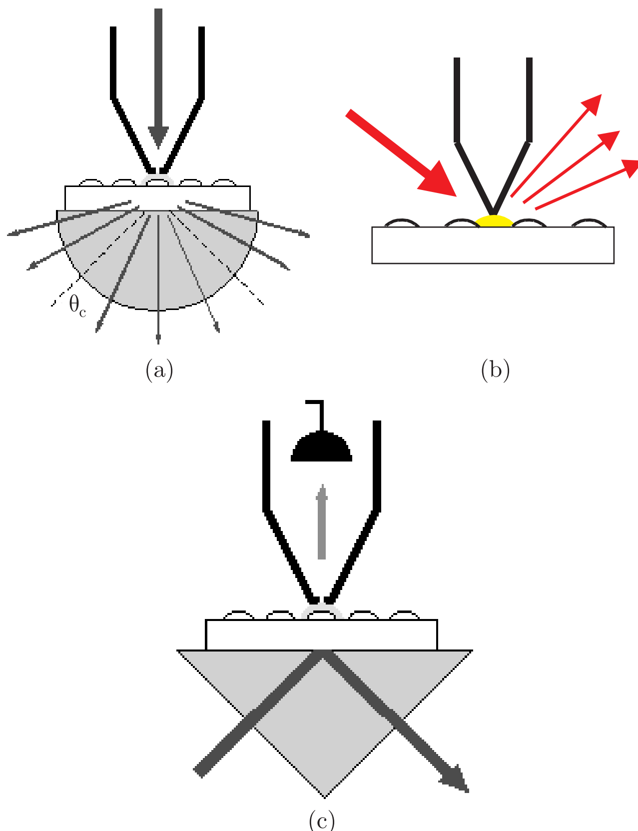


Fig. 2. Different types of SNOM. Aperture SNOM: reflection, transmission (allowed and forbidden light detection) or collection mode a); apertureless SNOM (light scattering by sharp tip) b); PSTM configuration (photon tunnelling) c)

## 3. PSTM system

Photon Scanning Tunnelling Microscope (PSTM) is optical analog of STM (Scanning Tunnelling Microscope). The last one employs a phenomena, consisting in exponential probability decay for electron tunnelling from conductive sample to a metallic tip through an insulating medium (air, vacuum). The tip plays a role of a local probe scanned on a distance of a few nm away from the surface. The electric signal (tunnel current) is kept constant by a piezoelectric transducer moving the tip closer or farther from the surface. Electric signal used for piezotransducer control reveals information on the sample surface topography. In PSTM exponentially decreasing intensity of optical field due to total internal reflection (TIR) from the scanned surface is employed to produce required information [15,16]. It is called evanescent field. The optical point probe in the form of tapered waveguide is immersed into evanescent field. The second end of the fibre is coupled to light detector (photodiode, photomultiplyer). Detector current can be written as:

$$I = I_0 \exp(-2qZ) + I_s$$

where:

$$q = k\left\{(n_2/n_1)^2 \sin^2\theta - 1\right\}^{1/2}$$

and:

$k$ – is magnitude of the wave vector of incident light,
$I_0$ – is detector current with waveguide tip placed in the sample plane,
$I_s$ – is scattered light detector current,
$Z$ – is tip-sample distance,
$n_0, n_1$ – are refractive indices of materials,
$\theta$ – is angle of light incidence.

Since the waveguide tip end diameter is typically 50 nm, the lateral resolution is approximately the same. The vertical resolution depends on decay length and this relays on material configuration, light wavelength and angle of light incidence. In typical situation it equals a few nm.

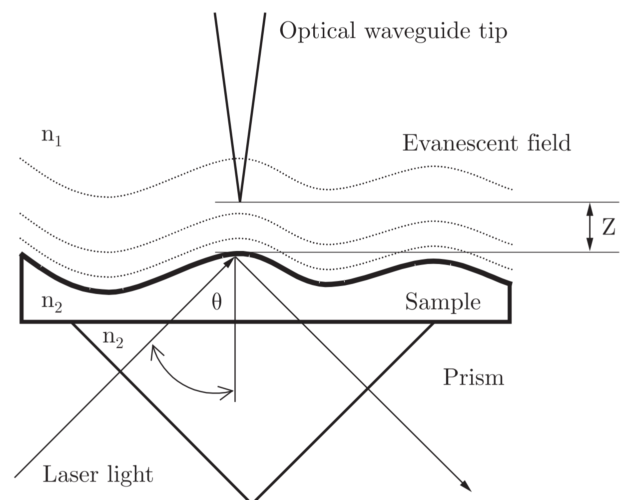


Fig. 3. Principle of the PSTM operation

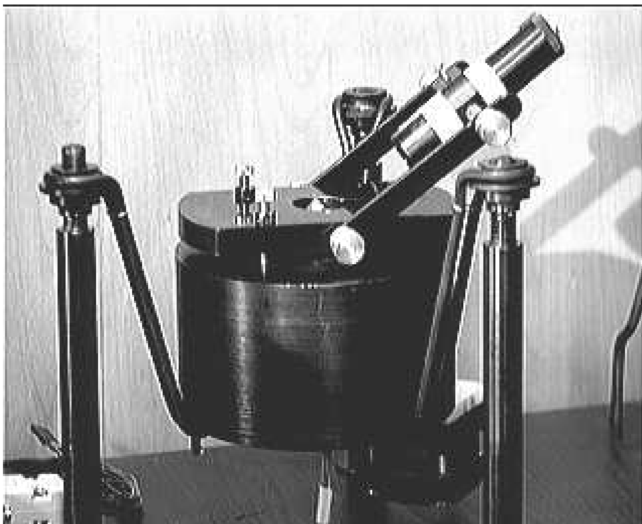

(a)

(b)

Fig. 4. PSTM head constructed at Wrocław University of Technology: overview a), hinged flap with prism sample holder details b)

Typical configuration of PSTM is shown in Fig. 3. Just as in STM, the tip in the PSTM is scanned with tubular piezoelectric scanner with feedback electronics to maintain a constant photocurrent. Optical signal coupled to the detector is very week (usually at the range of a few pW of optical power) and the detection system should be carefully designed to obtain a proper signal to noise ratio [17]. The mechanical design of microscope head is illustrated in Fig. 4. It consists of semiconductor laser light source with $\lambda = 630$ nm, heavy head body with tubular 4-electrode scanner for X,Y,Z precise sample movement and hinged flap which can be tilted by micrometer screws for rough tip movement. Prism with sample holder is placed in the centre part of the flap. The rest of the system is almost the same as in STM systems.

**3.1. Technology of the tips.** The main problem in PSTM is technology of the tips. The measured signal includes not only the optical tunnelling component. The main disturbance comes from the light scattered from surface roughness and dust particles. For tip-sample distances bigger than decay length of evanescent field scattered light becomes dominant in the measured signal as illustrated in Fig. 5. The tips are usually produced from monomode optical waveguides by chemical etching. In our laboratories we used 125 µm SM600 single mode fibre produced by YORK Company. The first step was the same as that reported in [18]. A polymer fibre cover was removed at distance of 2 cm from the end of 1 m long fibre which was carefully cleaved to obtain perpendicular end face. After cleaning in ultrasonic bath with pure acetone the end of the fibre was immersed into 48% solution of hydrofluoric acid covered with silicon oil. The temperature was kept at 70°C during the etching. After approx 10 min. the immersed part of the fibre was completely etched, making this way a tip that was ready for the next technological step. Figure 6 (a and b) is the SEM picture of obtained tip. As it is seen from the SEM pictures, etching process is self-centring due to slower etching speed of Ge doped waveguide core. We achieved tips with diameters down to 50 nm with sides smooth enough to reduce scattered light collecting. Tip was short (approx 3 times the diameter of the fibre) and mechanically stable. The next technological step was vacuum evaporation of aluminium onto the sides of the prepared tip. We used standard oil vacuum evaporation equipment. The fibre was fixed under vacuum chamber with axis tilted in respect to metal vapour source. That was done in order to leave an aperture on the very end of the tip. During evaporation the fibre was rotated axially. The SEM picture of the tip after Al coating is presented in Fig. 6c. Dark spot on the tip end with diameter approx 50 nm is the non covered part of a prepared fibre probe.

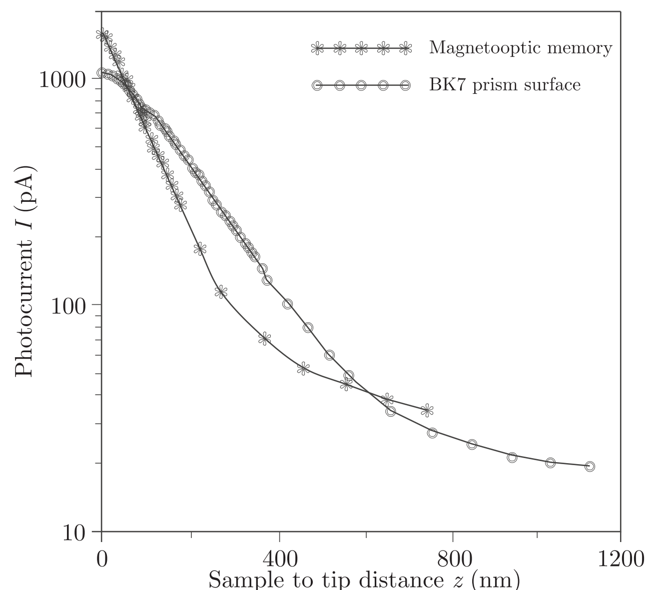


Fig. 5. Optical signal versus tip-sample distance for two materials with different refractive indices. Left part of both curves are following eq. 1 (dominated tunnelling phenomena). Right parts with decreasing slope are affected by scattered light coupled directly to the tip

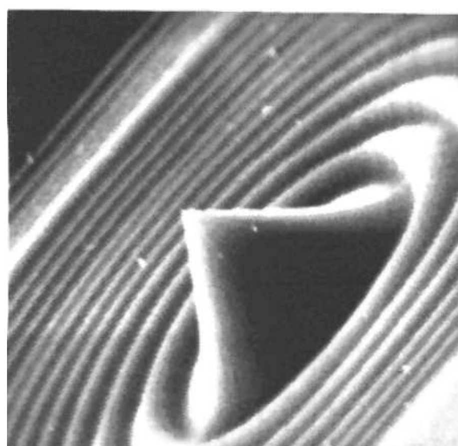

(a)

(b)

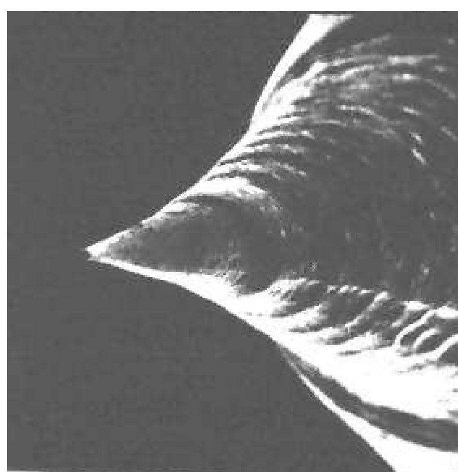

(c)

Fig. 6. SEM pictures of the intermediate (a, b) and final stage of the fibre tip preparation (c). The fibre have been etched 48% HF acid kept in 70°C covered by silicon oil film. Finally it have been covered with Al layer in standard vacuum evaporation system

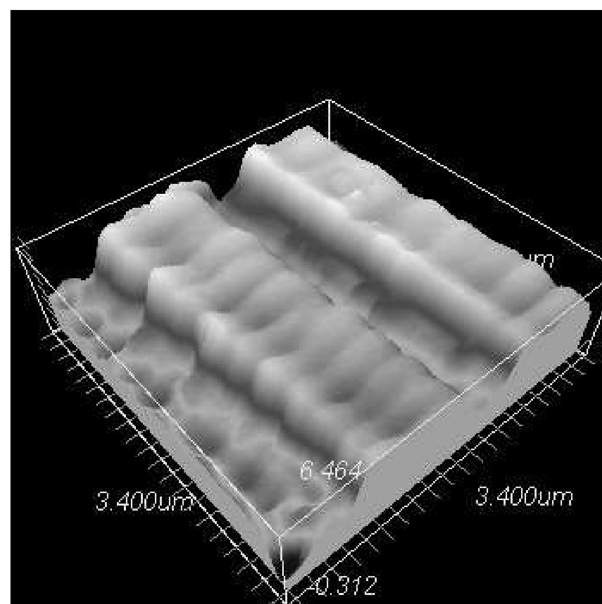


(a)

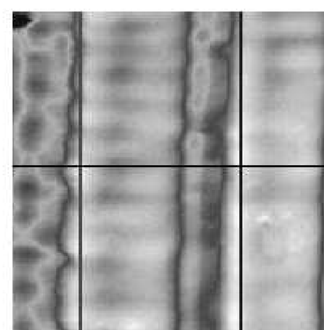

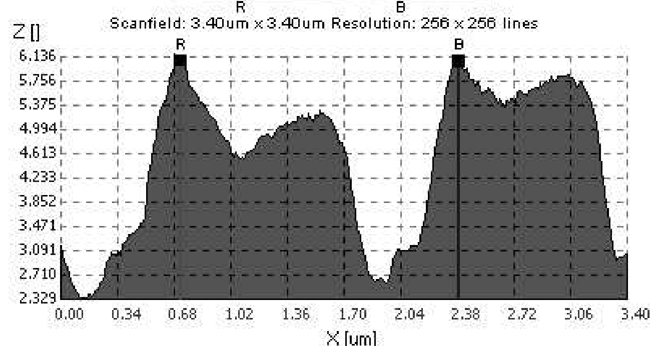


(b)

Fig. 7. 3D picture a) and cross-section b) of MO storage disc topography taken with tip from fig. 6b). The image size is equal 3.4 × 3.4 µm, structure height is 140 nm

**3.2. Experimental results.** The tips prepared as above are used as point probes in the laboratory made photon scanning tunnelling microscope (Fig. 4).The arrangement of the tip, the sample and the light source (semiconductor laser, $\lambda = 630$ nm) is similar to that reported in the literature [15,19]. Figure 7 illustrated obtained topography image of MO storage disc topography taken with tip from Fig. 6b. As the tip slopes are smooth, tip is rather short and the apex position is in the centre of waveguide core, the image is almost free from scattered light influence in respect to the images taken with tips prepared without oil on the etchant surface or by pulling method [18]. The strips surface visible in Fig. 7 is almost flat following real

structure. But still there is another effect. Looking at the cross-section line in Fig. 7b we notice that the structure is asymmetrical. The left slopes are higher than the right ones. This is an influence of laser light direction which has been perpendicular to the groove direction during measurements. In that case the total internal reflection is not valid in all surface points rendering to possible a direct light coupling from the structure under test to the tip via uncovered waveguide core on the slope of the tip. In Fig. 8a topography of CD disc surface is shown. It is taken by tip from Fig. 6c. Since the tip slopes are covered by aluminium layer at that time the light direction is not a problem. Even round shaped details on the sample surface can be monitored due to the shield effect of the metal layer. Although the images are good enough there are still some disadvantages of chemical etched wavegiude tips. The microscopic roughness of the glass surface on the tip sides leads to metal coating imperfections and even pinholes which renders it possible to collect non NFO signals. It is clearly visible in Fig. 8 at right side of the image as a artifact wavy structure. The next disadvantage of fibre tips is a limited transmission coefficient of an aperture probe at a given wavelength due to squeezing of the light wave passing through tapered metal covering waveguide subwavelength region. For typical tips with taper angle of 30° and 50 nm aperture on the end of the aperture throughput is about $10^{-6}$.

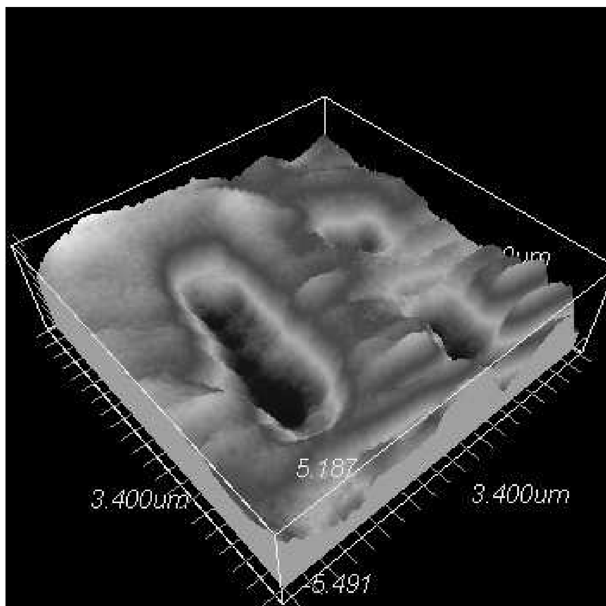


Fig. 8. 3D picture of CD disc topography taken with tip from Fig. 6c. The image size is equal to $3.4 \times 3.4$ µm, structure height is 145 nm

## 4. SNOM system

In general, optical signal itself can be used to regulate the distance between sample and the tip. However every non-transparent obstacle laying on the surface decreasing optical signal will be interpreted by feedback loop as an increase of tip-sample distance. As a consequence the system will decrease the distance crashing the tip. Having in mind all disadvantages we elaborated a combination of nanoaperture transmission (SNOM) with integrated deflection detector AFM cantilever. Figure 9 illustrated a concept of such a device.

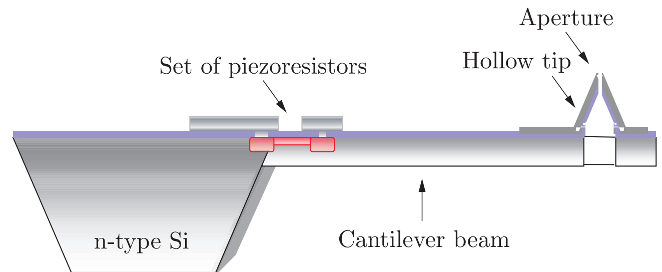


Fig. 9. Concept of SNOM-probe integrated into piezoresistive cantilever

**4.1. Technology of SNOM/AFM cantilevers.** The best known setup of the cantilever with integrated deflection detector was described by Tortonese et al. [20]. In this construction the U-shaped cantilever contains the piezoresistive deflection sensor. The mechanical stress occurring by the cantilever bending changes the resistance of the piezoresistor. In our design the piezoresistive detector contains four piezoresistors that form a Wheatstone bridge [21]. This solution ensures higher efficiency of piezomechanical transformation and thermal stability. When the cantilever is bent by a force acting on beam tip the maximum (minimum) mechanical stress appears on the supporting point of the beam. To obtain maximal sensitivity the piezoresistive Wheatstone bridge is located in the crystal direction [10] on the supporting point of the cantilever. Modification of this design also enables us to measure a lateral forces in Lateral Force Microscopy [21].

In presented cantilever construction a highly reproductive batch processing have been used to integrate both, cantilever playing role of an AFM detector and nanoaperture SNOM detection. [22, 23]. Produced cantilever with piezoresistors and hollow metal pyramid on the end is shown in Fig. 10. The nanoaperture with diameter of 50 nm have been formed by a direct ion beam drilling technique. We used a focused beam of 30 keV Ga+ ions and dose of about $2 \times 10^9$ ions. Because cantilevers are produced in form of regular array (mass production from silicon wafer) the position of ion beam can be dialled in automatically enabling rapid processing of the sample. The available FIB systems equipped with an $x - y$ stage and image recognition system allows drilling 360 sensor chromium pyramids on the wafer at a reasonably short time with an excellent reproducibility. Creation of a small aperture is the last step of the SNOM/AFM microprobe fabrication.

**4.2. Experimental results.** Prior to using fabricated probes in SNOM/AFM system we tested its throughput and polarization behaviour. We tested them in far field using 0.5 $NA$ microscopic objective at helium-neon laser light ($\lambda = 0.6328$ µm) with beam power of $P = 5$ mW. The input polarization was controlled using half- and quarter-wave plates. The degree of polarization after beam passing the nanoaperture under test

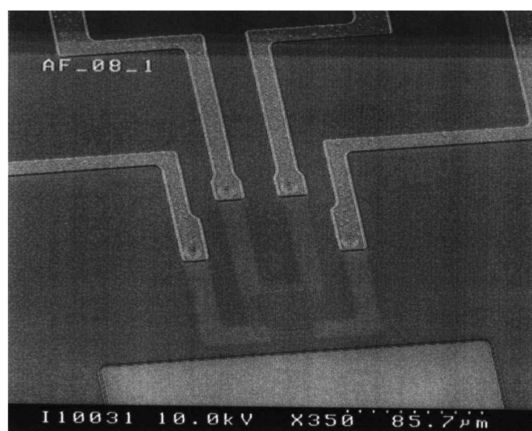


(a)

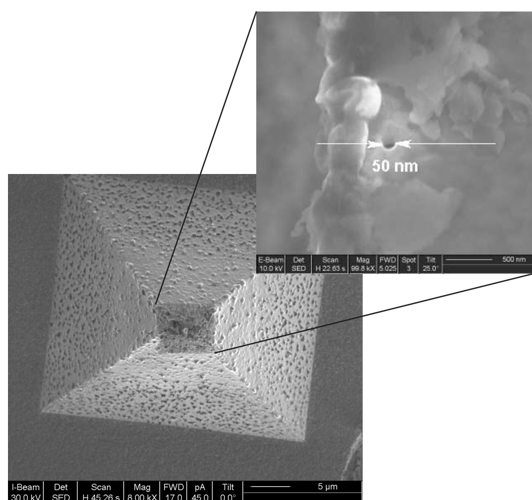


(b)

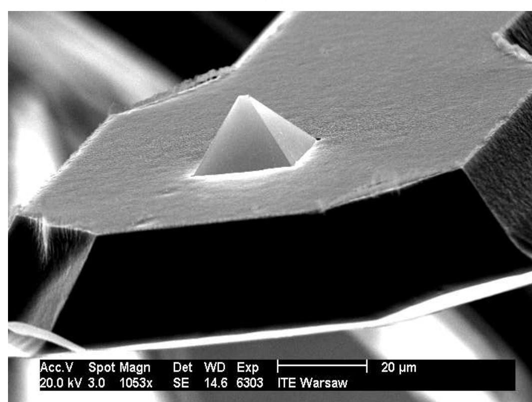


(c)

Fig. 10. SNOM/AFM microprobe integrated with piezoresistive cantilever beam- SEM image of piezoelectric deflection sensor (a), the pyramid tip with aperture (b) and the beam end with pyramid (c)

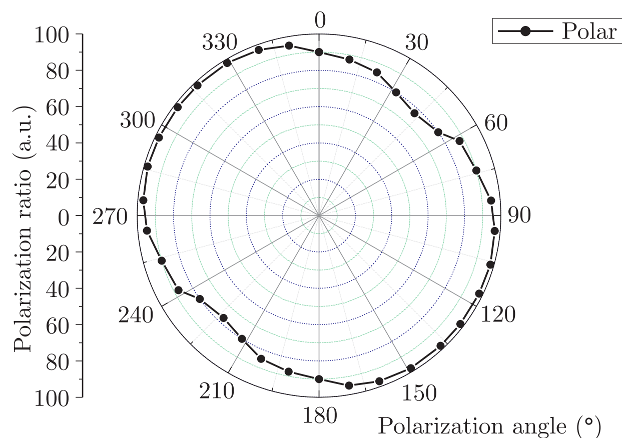


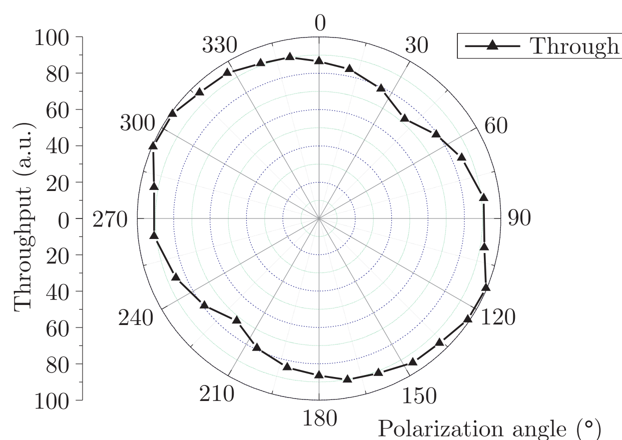


Fig. 11. Polarization ratio (a) of 50 nm aperture from Fig. 10a and its throughput ratio (b)

was measured by analyzer placed just before detector plane. In Fig. 11a) we show polarization graph of the aperture from Fig. 10b). We found out that the minimum polarization ratio was about 1 : 77 and maximum about 1 : 98. The difference between maximum and minimum polarization ratio is less than a factor of 1.27 which is involved by excellent circularity of the aperture opening formed by FIB technique (smaller factor denotes better symmetry of aperture optical properties). The similar measurements were done on FIB etched SNOM tips [24], fabricated from optical fibres by pooling process which gave polarization ratio typically exceeding 1 : 40 with polarization ratio difference less then the factor of 3. It means that our SNOM/AFM microprobe apertures are much more symmetrical. Fig 11b denotes that throughput of the aperture is in the range of 30% in respect to the polarization direction. Its maximum value equals to $5 \times 10^{-5}$ which is a very good result for 50 nm aperture. SNOM fibre tips, reported in [24], have throughput of about $10^{-5}$ at 90 nm aperture. Basing on calculation done in [25] we can estimate that the factor will be $10^{-6}$ at 50 nm for SNOM fibre tips. Our SNOM/AFM microprobe tips will deliver much higher optical signal then reported in [24]. According to our knowledge described measurements of SNOM/AFM microprobe aperture quality have never been done by other researchers.

Produced cantilevers have been used in home build AFM system with some extras enabling for SNOM operation [26]. Figure 12 presents 3D SNOM image of latex spheres shadows. The samples were prepared using aqueous suspension of polystyrene latex spheres. We used triply distilled water with SDS (0.0025% sodium dodecyl sulfate) as a surfactant. In order to obtain a uniform layered structure of latex spheres, the surface of substrate should be hydrophilic (must be wetted by the solution). We used freshly cleaved mica on which spread-

out solution forms a thin film. Upon drying at ambient temperature, the solution evaporates from surface, the capillary force pulls the spheres together and film of spheres is formed. 1 μm latex spheres on mica surface were covered with an evaporated 20 nm Al layer. The spheres were then removed with methanol in ultrasonic bath cleaner leaving Al triangular-shaped shadows on the mica substrate. Latex spheres form a hexagonal close-packed lattice (HCP) It is clearly seen analyzing Fig. 11 that optical image contains details smaller than 100 nm. The experiments performed shows the ability of our system to resolve objects of size close to nanoaperture diameter in optical domain.

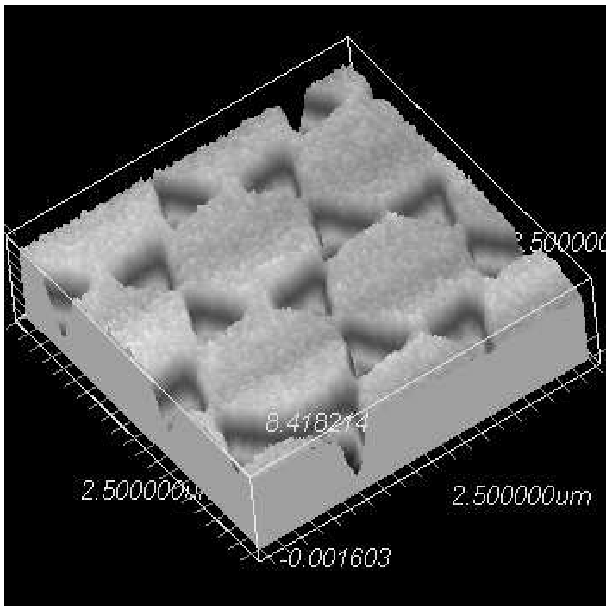


Fig. 12. 3D SNOM image of latex spheres shadows ($\Phi = 1\mu$ m) (Al on mica)

## 5. Conclusions

We have presented two systems of subwavelength resolution elaborated in our laboratory. The first – PSTM is based on point probes made by chemical etching of single mode optical waveguide. The elaborated tip technology renders it possible to observe samples topography with subwavelength resolution independently of surface shape. The second system is based on SNOM/AFM cantilevers with hollow tip with nanoapertures down to 50 nm drilled using FIB. The available FIB systems equipped with $xy$-stage and image recognition allows drilling 360 sensor Cr pyramids on wafer for reasonably short time with excellent reproducibility (size deviation and circularity). During measurements we found normalized polarization ratio values lying between $1 : 77$ and $1 : 98$. Thus, a very good optical properties of our SNOM/AFM cantilevers was confirmed. The transmission coefficient of nanoapertures throughput ratio was $5 \times 10^{-5}$ with values lying within 30% in respect to the polarization direction. Very good optical parameters of elaborated cantilevers with circular apertures makes them very interesting for polarity dependent experiments which will be performed in near future.

**Acknowledgments.** Author would like to express many thanks to P. Grabiec, K. Domanski, M. Zaborowski for help with cantilever technology, T. Schenkel for performing FIB ion drilling of nanoapertures and T. Gotszalk for measurements of cantilever mechanical parameters and many useful discussions.

References

[1] R. Hooke, *Micrographia or Some Physiological Descriptions of Minute Bodies Made by Magnifying Glasses with Observations and Inquiries Thereupon*, London, 1665.

[2] E. Abbe, "Beitraege zur Teorie des Microskops und der Microskopischen Wahrnehmung", *Arch. Mikroskopische Anatomie* 9, 413 (1873).

[3] J.W. Strutt (Lord Rayleigh), "Investigations in optics with special reference to the spectroscope", *Phil. Mag.* 8, 261–274 (1879).

[4] K. Visscher, *Optical Micromanipulation and Confocal Microscopy*, Amsterdam, Universiteit van Amsterdam, 1993.

[5] M. Minsky, "Memories on inventing the confocal scanning microscope", *Scanning* 10, 128–138 (1988).

[6] E.H Synge, "A suggested model for extending microscopic resolution into ultra-microscopic region", *Philos. Mag.* 6, 356–362 (1928).

[7] D.W. Pohl, W. Denk, and M. Lanz, "Optical stethoscopy: image recording with a resolution $\lambda$/20", *Appl. Phys. Lett.* 44, 651–653 (1984).

[8] A. Lewis, M. Isaacson, A. Harootunian, and A. Muray, "Development of a 500 Å spatial-resolution light-microscope", *Ultramicroscopy* 13, 227–231 (1984).

[9] Th. Enderle, T. Ha, D.S. Chemla, and S. Weiss, "Near-field fluorescence microscopy of cells", *Ultramicroscopy* 71, 303–309 (1998).

[10] M.F. Garcia-Parajo, J.A. Veerman, A.G.T. Ruiter, and N.F. van Hulst, "Near-field optical and shear-force microscopy of single fluorophores and DNA molecules", *Ultramicroscopy* 71, 311–319 (1998).

[11] V. Deckert, D. Zeisel, R. Zenobi, and T. Vo-Dinh, ", Near-field surface-enhanced Raman imaging of dye labelled DNA with 100 nm resolution", *Anal. Chem.* 70, 2646–2650 (1998).

[12] A. Hartschuh, N. Anderson, and L. Novotny, "Near-field Raman spectroscopy using a sharp metal tip", *J. Microsc.* 210, 234–240 (2003).

[13] T. Ha, T. Enderle, D. S. Chemla, P. R. Selvin, and S. Weiss, "Single molecule dynamics studied by polarization modulation", *Phys. Rev. Lett.* 77, 3979–3982 (1996).

[14] X.K. Orlik, M. Labardi, and M. Allegrini, "Nanometer scale observation of ferroelectric domains using an apertureless near field optical microscope", *Appl. Phys. Lett.* 77, 2042–2044 (2000).

[15] R.C. Reddick, R.J. Warmack, and T.L. Ferrell, "New form of scanning optical microscopy", *Phys. Rev.* B 39 (1), 767–770 (1989).

[16] H. Pagnia, J. Radojewski, and N. Sotnik, "Operation conditions of an optical STM", *Optik* 86 (3), 87–90 (1990).

[17] J. Radojewski and T. Gotszalk, "Optical signal detection problems in photon scanning tunneling microscope (PSTM)", *Proc. ISHM Poland Chapter Conference*, 255–258 (1996).

[18] J. Radojewski, N. Sotnik, and H. Pagnia, "Tip technology for optical scanning tunneling microscopy and its influence on image quality", *Int. J. of Electronics* 76 (5), 973–980 (1994).

[19] D. Courjon, K. Sarayeddine, and M. Spayer, "Scanning tunneling optical microscopy", *Optics Communications* 71, 23–28 (1989).

[20] M. Tortonese, R.C. Barett, and C.F. Quate, "Atomic resolution with an atomic force microscope using piezoresistive detection", *Appl. Phys. Lett.* 62 (8), 834 (1993).

[21] T. Gotszalk, P. Grabiec, and I.W. Rangelow, "Piezoresistive sensors for scanning probe microscopy", *Ultramicroscopy* 82 (1–4), 39 (2000).

[22] P. Grabiec, T. Gotszalk, J. Radojewski, K. Edinger, N. Abedinov, and I.W. Rangelow, "SNOM/AFM microprobe integrated with piezoresistive cantilever beam for multifunctional surface analysis", *Microelectr. Eng.* 61–62, 981–986 (2002).

[23] P. Grabiec, J. Radojewski, M. Zaborowski, K. Domański, T. Schenkel, and I.W. Rangelow, "Batch fabricated scanning near-field optical microscope/atomic force microscopy microprobe integrated with piezoresistive cantilever beam with highly reproductible focused ion beam micromachined aperture", *J. Vac. Sci. Technol.* B 22 (1), 16–21 (2004).

[24] J.A. Veerman, A. M. Otter, L. Kuipers, and N.F. van Hulst, "High definition aperture probes for near-field optical microscopy fabricated by focused ion beam milling", *Appl. Phys. Lett.* 72 (24), 3115–3117 (1998).

[25] B. Hecht, B. Sick, U.P. Wild, V. Deckert, R. Zenobi, O.F. Martin, and D.W. Pohl, "Scanning near-field optical microscopy with aperture probes: Fundamentals and applications", *J. Chem. Phys.* 112 (18), 7761–7774 (2000).

[26] J. Radojewski and P. Grabiec, "Combined SNOM/AFM microscopy with micromachined nanoapertures", *Materials Science* 21 (3), 319–332 (2003).